Available online at www.sciencedirect.com
ScienceDirect
Optical Materials 29 (2007) 619–622
OPTICAL Materials
www.elsevier.com/locate/optmat

Porous silicon based narrow line-width rugate filters

S. Ilyas [a], T. Böcking [a], K. Kilian [b], P.J. Reece [a], J. Gooding [b], K. Gaus [c], M. Gal [a,*]

[a] School of Physics, University of New South Wales, Sydney 2052, Australia
[b] School of Chemistry, University of New South Wales, Sydney 2052, Australia
[c] Centre for Vascular Research, School of Medical Sciences, University of New South Wales, Sydney 2052, Australia

Received 23 June 2005; accepted 11 October 2005
Available online 3 January 2006

Abstract

We report on the design and fabrication of porous silicon based rugate filters. We have achieved narrow line-width, high reflectivity optical filters made entirely from silicon by continuously varying of the refractive index of Si and apodizing the index profile of the structure.

Keywords: Optical filter; Porous silicon; Rugate filter

1. Introduction

Rugate filters are a class of optical filters that contain a *continuous* variation of the refractive index, usually sinusoidal, in the direction perpendicular to the plane of the filter [1–3]. The reflectance of such a filter shows a high reflectivity "stop-band" around a characteristic wavelength, λ_0, and very low reflectivity elsewhere. Such filters can be used, for example as single line stop-band filters, in various sensor applications, etc. Rugate filters are often preferred over conventional step-index multilayer filters because they do not display higher order harmonics. In addition, by combining several different sinusoidal refractive index distributions, rugate filters can be made to reproduce unusual or difficult optical response functions which are not possible using simple step-index profiles [1]. On the other hand, such filters are difficult to fabricate because the continuous refractive index profile necessitates continuous variation in the density and/or composition of the filter material. Several techniques have been tried in the past, including evaporation, reactive sputtering, and plasma-enhanced vapour deposition [4–6]. Although rugate filters can be, and have been made using these techniques, such methods require complex equipment and are time-consuming. Berger et al. [7] reported a simpler and quicker method for the fabrication of rugate filters using electrochemical etching of silicon. These types of filters were recently discussed in detail by Lorenzo et al. [8]. During electrochemical etching of silicon, the density of the generated porous silicon can be continuously varied, making it possible to generate continuously varying refractive index distributions in the direction perpendicular to the plane of the filter. In these types of filters the layers are etched into the substrate rather than being deposited on top of it. If necessary, the filters can be detached (lifted off) from the substrate during the final stages of the electrochemical etching process, to become a free-standing thin film filter or can be attached to a glass substrate. In addition to being inexpensive and relatively easy to make, porous silicon based devices have the added advantage of being compatible with silicon opto-electronics and could be part of future Si integrated optical system [9–12].

The rugate filters described by Berger et al. [7] and Lorenzo et al. [8] had relatively large stop-bands. While stop-bands of several hundred nanometers are adequate or even desirable in some applications, our interest in optical sens-

* Corresponding author. Tel.: +61 2 9385 4549; fax: +61 2 9385 6060.
E-mail address: m.gal@unsw.edu.au (M. Gal).

0925-3467/$ - see front matter © 2005 Elsevier B.V. All rights reserved.
doi:10.1016/j.optmat.2005.10.012

ing necessitated the development of narrow line-width rugate filters that could be used to detect small changes in the refractive index of the filter. In this study, therefore we describe our approach and our results in making narrow line-width rugate filters operating in the sub 1 μm spectral region using porous silicon.

2. Theory

Rugate filters were made by sinusoidally varying the refractive index of the material in the direction perpendicular to the plane of the filter. The refractive index profile, $n(x)$, of a rugate filter centered on λ_0 can be written in the following form:

$$n(x) = n_0 + \Delta n/2 \sin(4\pi x/\lambda_0)$$

where x is the perpendicular distance into the plane of the filter, n_0 is the average refractive index, and Δn is the refractive index contrast [1,13,14]. For small index contrast, such a sinusoidal profile would result in the reflection spectrum displaying a single stop-band at λ_0, the bandwidth of which is a function of Δn. However, as a result of the sharp truncation of the refractive index modulation at the boundaries of the filter, a simple sinusoidal index profile would also generate interference oscillations appearing on both sides of the stop-band ("side lobes"). To suppress these unnecessary side lobes, the abrupt termination of the index profile has to be faded out or apodized with a smooth envelope function so as to reduce the index contrast to zero at the two boundaries of the filter. Of the various types of envelope functions that can be used for apodization, we chose to use a Gaussian function which resulted in the significant reduction of the side lobes while at the same time not affecting the optical properties of the stop-band. However, there is another reason for the existence of side lobes. The whole filter can be considered as a single layer with an average refractive index and an effective thickness, and will therefore produce interference oscillations corresponding to such a layer. To minimize this effect, the refractive indexes at the front and back of the filter have to be matched to air and the Si substrate respectively, to compensate for the mismatch between the average index of the filter and the surrounding media. This can be achieved by growing two additional continuously varying refractive layers that match the refractive indexes of the surface and the substrate.

A graphical illustration of the refractive index profile is shown in Fig. 1. The index profile includes the amplitude modulated sinusoidal refractive index (using Gaussian apodization) and two third-order polynomial index matching layers at the front and substrate end of the filter. In the example to be discussed below, the filter included 40 sinusoidal periods with an index contrast of $\Delta n = 0.028$ ($n_{HI} = 2.122$ and $n_{LO} = 2.094$). The index matching layer at the surface was designed to have a thickness of 450 nm, and the refractive index that smoothly decreased from 2.094 to 1.471 (which is the lowest refractive index

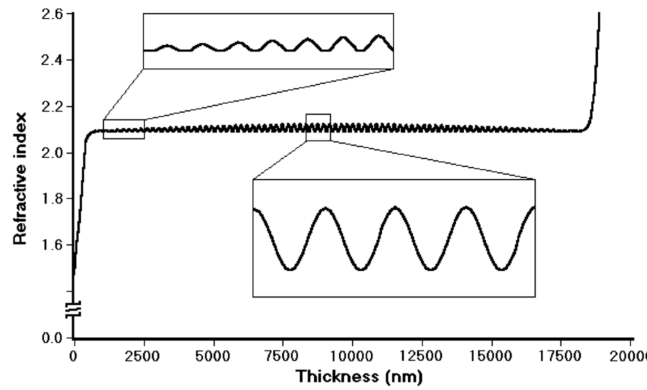

Fig. 1. Refractive index distribution of our filters, having amplitude modulated (apodized) sinusoidal refractive index with index matching layers at the front and the substrate end of the filter. The inserts show the apodization of the index, and the sinusoidal variation as a function of depth.

value we could achieve). The index matching layer at the Si substrate side was 675 nm thick, and the refractive index increased from $n = 2.094$ to $n = 3.5$ as a third-order polynomial.

The reflectivity spectrum of a filter having an index profile as shown in Fig. 1 was calculated using the characteristic matrix method [14,15], and is shown in Fig. 2. As can be seen, the chosen conditions lead to a stop-band at 850 nm

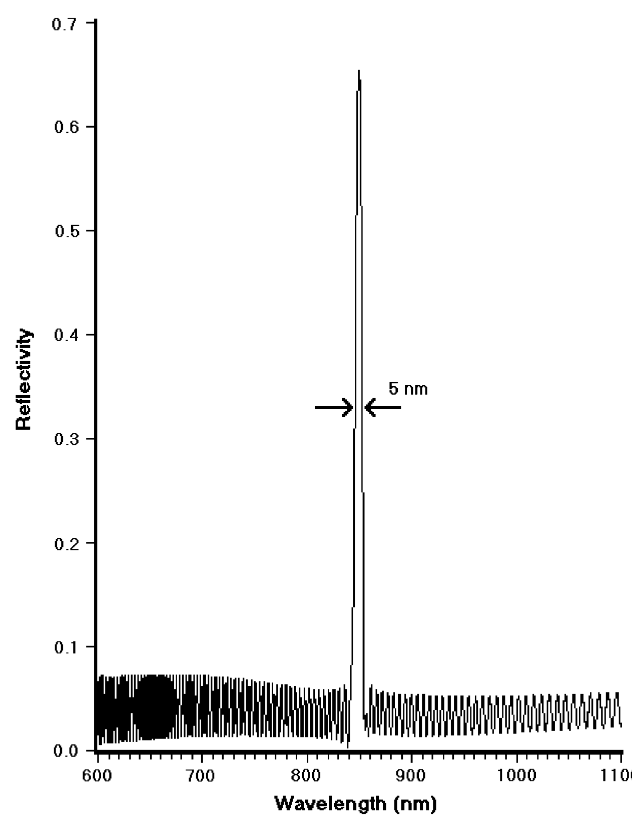

Fig. 2. Calculated reflectivity spectrum of a rugate filter assuming 40 sinusoidally varying refractive index layers, Gaussian apodization and index matching layers at the surface and substrate ends.

with a FWHM of approximately 5 nm, and a maximum reflectivity of 65%. The reflectivity outside the stop-band is predicted to be less than 10%. A porous silicon filter with these qualities is eminently suitable for biosensing applications.

3. Experimental results

Porous silicon (PSi) is a versatile material with a number of valuable optical properties. Although attention to nanostructured PSi originated with the discovery of visible room temperature photoluminescence [16], so far the most interesting applications of PSi are associated with passive multilayer optical devices. The refractive index of porous silicon is a function of the porosity of the material which, in turn is a function of the current density applied during formation of PSi. It is possible to fabricate intricate photonic structures on Si wafers just by varying the etching current during PSi formation. Using this method, a range of valuable optical devices have been made from PSi, such as optical microcavities, Bragg mirrors and waveguides [9,17]. Recently, we have used a *low temperature* fabrication technique to improve the optical quality of the PSi layers, and have made high quality optical devices, including omnidirectional mirrors, laser mirrors and sub-nanometre line-width optical cavities [10,11]. At low temperatures, a decrease in the ion mobility causes a higher rate of electropolishing, which tends to smooth out the inhomogeneities at the interfaces resulting in less scattering and hence better optical quality devices [18,19].

The rugate filters described in this report were prepared from highly boron doped p^+-type (1 0 0) silicon wafers having a resistivity of 0.07 Ω cm. The Si substrate was electrochemically etched at room temperature in a solution of 25% HF. This etching solution was prepared by diluting 48% HF solution into ethanol. The current density was varied between 2.205 mA/mm^2 and 2.256 mA/mm^2. During the etching process temporal breaks of 9 s were used at each sinusiodal period during the anodization to recover the HF concentration at the dissolution front. After the etching process, the samples were rinsed with ethanol, or used pentane drying to minimize the effects of capillary pressure within the porous structure.

To etch the required apodized sinusoidal index profile into Si, the etching current was computer controlled via the power supply (Keithley Source Meter 2400). We designed a small program based on National Instrument LabVIEW 6.1 such that each sinusiodal period was approximated by a number of step-functions, as shown in Fig. 3(a). Although the number of steps could be varied, we typically used 16 steps per period. Fig. 3(b) shows the current profile against time. The etch breaks are also shown in the figure (e.g. t2–t3). Increasing the number of steps up to 32 did not affect the outcome. The same computer program could also simulate the expected reflectivity spectra produced under the specific etching conditions.

The reflectivity spectrum of the filter described in Fig. 1 is shown in Fig. 4. The reflectivity was measured at normal incidence using a Spex 0.22 m spectrometer and Si detector. The reflectivity measurements were taken over an area of 0.5 mm^2, with a collection angle of 2.7°. As can be seen, the agreement between the calculated and measured spectra is very good. The measured spectrum has a stop-band at 848 nm, maximum reflectivity 63%, line-width 11 nm.

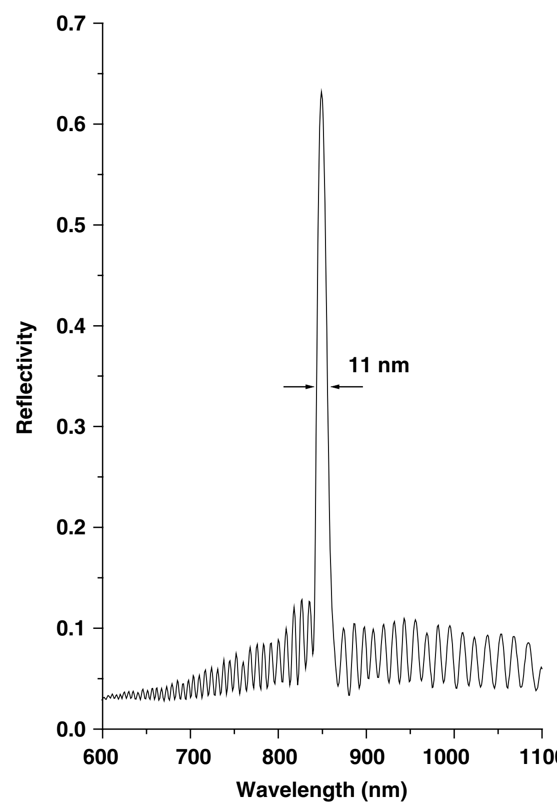

Fig. 4. Measured reflectivity spectrum of a filter having a refractive index profile shown in Fig. 1.

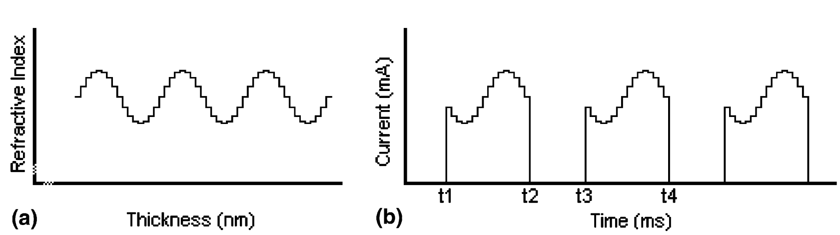

Fig. 3. Step-functions used to approximate the sinusoidal variation of refractive index.

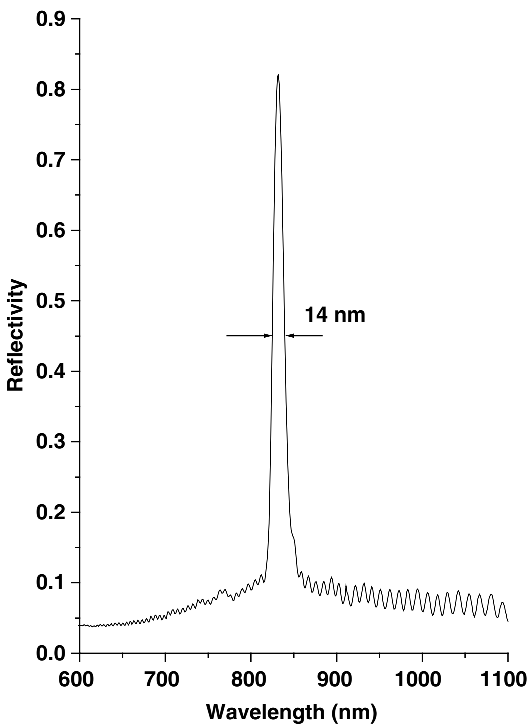

Fig. 5. The measured reflectivity spectrum of a filter having a refractive index profile similar to that shown in Fig. 1 and containing 100 sinusoidally varying refractive index layers.

The reflectivity outside the stop-band is less than 10%. These value are very similar those predicted by the theory.

There are two noteworthy differences between the measured and the calculated spectra: a slight increase in the line-width (from 5 nm to 11 nm), and exponentially decaying oscillations below approximately 800 nm. The increased line-width is most likely caused by small fluctuations in the porosity of the layers. The 5 nm line width was calculated assuming an index contrast of $\Delta n = 0.028$ which corresponds to a 1% variation in the porosity of the high and low index layers. Such small variations in porosity are difficult to maintain, and most likely the porosity variations are somewhat larger in the filter. The exponentially decaying interference oscillations below 800 nm are the result of the absorption of light in PSi, which was not taken into account in the calculations.

Another advantage of the PSi technology is the ease with which the number of layers can be increased. Increasing the number of layers from 40 to 100 is simple and only adds a few minutes to the overall fabrication time. Fig. 5 shows the measured reflectivity of a filter with the same index contrast ($\Delta n = 0.028$) but with 100 apodized sinusoidal layers. The peak reflectivity of this sample increased to 83%, and the average background reflectivity stayed below 10%, in agreement with theoretical predictions. The FWHM of the stop-band increased to 14 nm (from 11 nm) due to the slight variations in the porosity of the layers as discussed above.

When we kept the number of periods 100 but increased the porosity difference to 4%, which corresponds to a refractive index contrast of $\Delta n = 0.11$, the reflectivity maximum increased to over 99% with only a 4 nm increase in the line-width.

4. Conclusion

We have designed and fabricated narrow line-width porous silicon rugate filters that included continuously varying apodized refractive index profiles and index matching layers. The high reflectivity and narrow line-width of these filters make them ideal for sensor or line filter applications.

References

[1] B.G. Bovard, Applied Optics 32 (28) (1993).
[2] B.E. Perilloux, Thin Film DesignModulated Thickness and Other Stopband Design Methods, SPIE Press, 2002.
[3] F. Cunin et al., Nature 1 (2002).
[4] K. Kaminska, T. Brown, G. Beydaghyan, K. Robbie, Applied Optics 42 (20) (2003) 4212.
[5] K. Kaminska, M. Suzuki, K. Kimura, Journal of Applied Physics 95 (2004) 6.
[6] H. Bartzsch, S. Lange, P. Fracn, K. Goedicke, Surface and Coating Technology 180–181 (2004).
[7] M.G. Berger, R. Arens-Fischer, M. Thönissen, M. Krüger, S. Billat, H. Lüth, S. Hilbrich, W. Theiß, P. Grosse, Thin Solid Films 297 (1997) 237.
[8] E. Lorenzo, C.J. Oton, N.E. Capuj, M. Ghulinyan, D.N. Urrios, Z. Gaburro, L. Pavesi, Physical Status Solidi C 2 (9) (2005) 3227.
[9] O. Bisi, S. Ossicini, L. Pavesi, Surface Science Report 38 (2000).
[10] P. Reece, M. Zhang, G. Lerondel, M. Gal, Applied Physics Letters 81 (2002) 4895.
[11] W.H. Zheng, P. Reece, B. Sun, M. Gal, Applied Physics Letters 84 (2004) 3519.
[12] J. Volk, M. Fried, A.L. Toth, I. Barsony, Thin Solid Films 455–456 (2004) 535.
[13] N. Perelman, I. Averbukh, Journal of Applied Physics 79 (1996) 6.
[14] G.T. Dalakos, Computer Simulation of Rugate Optical Interference Filters by Using the Characteristic Matrix Method I: Introduction and Simple Application, General Electric Research and Development Center, 1999.
[15] H.S. Nalwa, Handbook of Thin Film MaterialsFerroelectric and Dielectric Thin Films, vol. 3, Academic Press, 2002.
[16] L.T. Canham, Applied Physics Letters 57 (1990) 1046.
[17] E.K. Squire, P.J. Russell, P.A. Snow, Applied Optics 37 (30) (1998) 7107.
[18] S. Setzu, S. Letant, P. Solsona, R. Romestain, J.C. Vial, Journal of Luminescence 80 (1999) 129.
[19] S. Setzu, G. Lérondel, R. Romestain, Journal of Applied Physics 84 (1998) 3129.